GEOPHYSICAL RESEARCH LETTERS, VOL. 40, 4260–4265, doi:10.1002/grl.50839, 2013

Bias in estimates of lithosphere viscosity from interseismic deformation

T. T. Hines[1] and E. A. Hetland[1]

Received 4 July 2013; revised 5 August 2013; accepted 6 August 2013; published 27 August 2013.

[1] The estimation of uniform viscosities representing the lower crust and uppermost mantle from postseismic or interseismic deformation (i.e., apparent viscosities) is inherently biased with respect to a depth dependence of the viscosities within each layer. Estimates are biased toward a more viscous lower crust or a less viscous lithospheric mantle, depending on the relative geometric mean viscosities of the two layers. When there is a low-viscosity shear zone beneath the fault, apparent viscosities are close to that of the shear zone immediately after the earthquake, although the apparent viscosities increase significantly during the later interseismic period. Inferences made from interseismic deformation that the lower crust is more viscous than the upper mantle may be entirely consistent with depth-dependent viscosity profiles that have a significant increase in viscosity from the lowermost crust to the uppermost mantle. **Citation:** Hines, T. T., and E. A. Hetland (2013), Bias in estimates of lithosphere viscosity from interseismic deformation, *Geophys. Res. Lett.*, *40*, 4260–4265, doi:10.1002/grl.50839.

1. Introduction

[2] Numerous studies in tectonically active regions have sought estimates of the viscosities of the ductile lithosphere, including the lower crust and uppermost mantle [e.g., *Hetland and Hager*, 2003; *Pollitz*, 2003, 2005; *Johnson et al.*, 2007; *Hearn et al.*, 2009]. Here we consider estimates of the ductile lithosphere made by fitting predictions of surface deformation from mechanical models to geodetic measurements of interseismic deformation, including both postseismic and interseismic deformation. Most studies of interseismic deformation concluded that the lower crust has a higher viscosity than the uppermost mantle [*Bürgmann and Dresen*, 2008; *Thatcher and Pollitz*, 2008]. The majority of mechanical models used in these studies approximated the ductile lithosphere using two homogeneous viscoelastic layers representing the lower crust and uppermost mantle [e.g., *Hetland and Hager*, 2003; *Pollitz*, 2003; *Hearn et al.*, 2009]. These simplistic layered models are commonly used because they are computationally cheap and because geodetic data are only capable of resolving a limited number of independent rheologic parameters [e.g., *Riva and Govers*, 2009; *Pollitz and Thatcher*, 2010]. However, the simplifications made in the layered models may result in inferred viscosities that are not directly applicable to the real viscosity structure of the ductile lithosphere [*Riva and Govers*, 2009].

[3] Temperature increases with depth and viscosity has a strong temperature dependence [e.g., *Kohlstedt et al.*, 1995]. The viscosity of the ductile lithosphere also has a stress dependence [*e.g.*, *Kohlstedt et al.*, 1995], although the ductile lithosphere is often approximated as Maxwell viscoelastic in these models [e.g., *Hetland and Hager*, 2003; *Johnson et al.*, 2007; *Riva and Govers*, 2009; *Yamasaki and Houseman*, 2012b]. This may be a reasonable approximation if stresses resulting from coseismic deformation are small compared to background stresses. The Newtonian viscosity inferred in postseismic deformation studies may not be constant over time and could be interpreted as an effective viscosity of a power law creep [e.g., *Freed et al.*, 2006]. Indeed, to describe geodetic observations, models of postseismic deformation in the months to years following an earthquake often require apparent viscosities up to several orders of magnitude smaller than those required in models of deformation later in the interseismic period [e.g., *Pollitz*, 2005; *Johnson et al.*, 2007; *Meade et al.*, 2013]. It is important to note that estimates of viscosities from the first few months following an earthquake may not be directly applicable to the steady viscosities of the lithosphere, as the immediate transient postseismic deformation is often considered to be due to postseismic fault creep, poroelastic rebound, or a transient rheology [e.g., *Pollitz*, 2003; *Freed et al.*, 2006; *Hearn et al.*, 2009]. We save the investigation of models with nonlinear, power law creep, and/or stress-driven fault creep to a subsequent study, and here we only consider stress-linear viscoelasticity, allowing for a robust depth dependence of viscosities.

[4] We address the question of how inferences of single viscosities representing the entire lower crust and uppermost mantle are related to depth-dependent viscosities throughout the ductile lithosphere. We consider inferred viscosities made from rheologically idealized models of interseismic deformation to be apparent viscosities and explore the biases incurred through using simplified models. For brevity, we use the term "strength" to refer to viscosity, or equivalently Maxwell relaxation time, τ_M ($\tau_M = \eta/\mu$, where η is viscosity and μ is shear modulus), and thus we use "strong" or "weak" to refer to high or low viscosities, respectively. We show that estimates of the lithosphere's strength, based on simplified layered models, are almost always biased toward a stronger lower crust or a weaker upper mantle.

2. Interseismic Models

[5] We create synthetic surface deformation using 2-D earthquake cycle models composed of an infinite length,

Additional supporting information may be found in the online version of this article.

[1]Department of Earth and Environmental Sciences, University of Michigan, Ann Arbor, Michigan, USA.

Corresponding author: T. T. Hines, Department of Earth and Environmental Sciences, University of Michigan, 2534 CC Little Bldg., 1100 N. University Ave., Ann Arbor, MI 48104, USA. (hinest@umich.edu)

0094-8276/13/10.1002/grl.50839

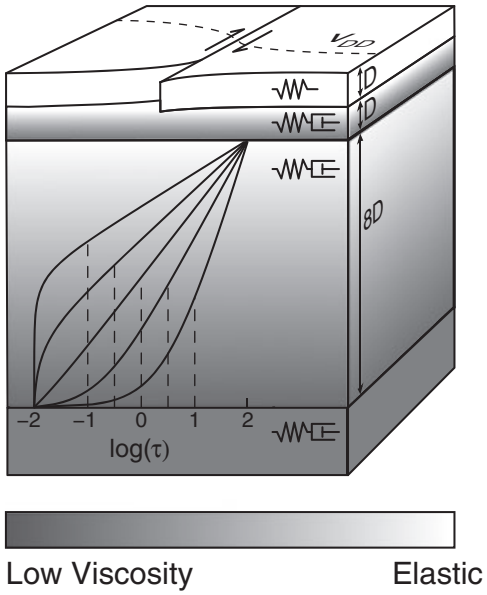

Figure 1. Schematic of the earthquake cycle model. Springs indicate elasticity and dashpots indicate Newtonian viscosity. Example depth-dependent τ profiles are shown in the upper mantle, for the case when $\tau_{UM}^{\min} = 10^{-2}$, $\tau_{UM}^{\max} = 10^{2}$, and $\bar{\tau}_{UM}$ indicated by vertical dotted lines.

vertical strike-slip fault in an elastic layer of thickness D representing the upper crust, overlying a Maxwell viscoelastic substrate representing the ductile lithosphere (Figure 1). We impose uniform slip on the fault with repeat time T, until the surface deformation reaches a cycle invariant state (i.e., the model is spun-up). The lower viscoelastic substrate is composed of a layer of thickness D, representing the lower crust, and a layer of thickness $8D$, representing the lithospheric mantle. We choose the thickness of the latter to be large enough such that the specific thickness does not affect the surface deformation. Below $10D$, in the asthenosphere, we assume a homogeneous viscosity of 10^{19} Pa·s to the base of the model domain. Models of infinite length, vertical strike-slip faults are antisymmetric, and we only model one side of the fault. We use the finite element program GeoFEST [*Lyzenga et al.*, 2000] and take the model domain to be $120D$ wide by $100D$ deep. We impose an antisymmetry boundary condition on the model edge containing the fault, a far-field velocity, v_T, on the opposite boundary, chosen so that there is no net strain accumulation in each earthquake cycle, and the top and bottom of the model are stress free (the bottom of the model domain is sufficiently deep that the bottom stress free boundary condition does not affect the surface deformation). We consider only Maxwell viscoelasticity but include depth-dependent viscosities within the lower crust and uppermost mantle. We assume that the shear modulus is uniform throughout the model and that viscosities vary smoothly, except possibly at $z = 2D$ (i.e., the Moho) and at $z = 10D$ (i.e., base of the lithosphere). We nondimensionalize the spatial dimensions by the fault locking depth, D, and time by T, and thus, the nondimensional Maxwell relaxation time is $\tau = \tau_M/T$.

2.1. Depth Dependence of τ

[6] Motivated by the fact that effective viscosity decreases exponentially with increasing temperature [e.g., *Kohlstedt et al.*, 1995], we take τ to decrease exponentially with depth. For generality, we do not assume any particular geotherm or composition of the ductile lithosphere and instead specify that τ decreases in each layer as

$$\tau(z) = \alpha + \beta e^{-\gamma z}, \tag{1}$$

where z is depth within the layer and α, β, and γ are parameters that vary for each layer. The parameters in equation (1) depend on the maximum, $\tau_j^{\max}$, minimum, $\tau_j^{\min}$, and geometric mean, $\bar{\tau}_j$, relaxation times within layer j, where j is "LC" or "UM" for the lower crust or mantle lithosphere, respectively. We consider a wide range of viscosity profiles such that $10^{-1} \le \tau_j^{\max} \le 10^{2}$, $10^{-2} \le \tau_j^{\min} \le 10^{1}$, and $10^{-1} \le \bar{\tau}_j \le 10^{1}$, in increments of $10^{0.5}$. With these ranges, we consider 5625 depth-dependent lithosphere viscosity structures. The relaxation times are nondimensionalized by T, so for a 100 year recurrence time, the shortest and longest Maxwell relaxation times we consider are 1 and 10^4 years, respectively (corresponding to viscosities of about 10^{18} and 10^{22} Pa·s for $\mu \approx 30$ GPa). Note that we consider profiles both in which the largest decrease of τ is predominantly in the top or bottom of the layer (Figure 1), and we remark on the impact of this on our results below.

3. Determination of Apparent Strength

[7] We define the apparent relaxation times (or equivalently the apparent viscosities) of the lower crust, $\hat{\tau}_{LC}$, and mantle lithosphere, $\hat{\tau}_{UM}$, as the relaxation times inferred from surface interseismic deformation using a model composed of constant viscosities in the two layers (i.e., a layered model). In general, $\hat{\tau}_{LC}$ and $\hat{\tau}_{UM}$ have a temporal [*Riva and Govers*, 2009] and spatial [*Yamasaki and Houseman*, 2012a] dependence. Both of which can be thought of as variables of interseismic surface deformation given a particular mechanical representation of the ductile lithosphere, but here we only consider the time dependence of inferred viscosities. We denote the interseismic surface velocities in the models with depth-dependent τ as v_{DD}, and the velocities in a layered model as v_L. We use a grid search to determine the $\hat{\tau}_j$ in a layered model that produced surface velocities that closest match the surface velocities in each of the depth-dependent models at 100 evenly spaced times throughout the interseismic period. In the grid search, we search over $10^{-2} \le \hat{\tau}_j \le 10^{2}$, minimizing the root-mean-square error (RMSE) between v_{DD} and v_L at $0.5D$ increments of distance from the fault from $0.5D$ to $12D$. We note that the upper limit of $\hat{\tau}_j$ searched over is a bit excessive because, for practical purposes, v_L is insensitive to changes in relaxation time for $\tau \gtrsim 10^{1}$, as the layer is effectively elastic over interseismic periods [*Savage and Prescott*, 1978] (Figure S1 in the supporting information). Finally, we assume that the fault slip rate and thickness of the lower crust and upper mantle are known.

[8] About halfway through the interseismic period, surface deformation for almost all models we consider, both layered and depth dependent, is indistinguishable from the deformation predicted by an elastic model with slip rate v_T and locking depth D [*Savage and Burford*, 1973] (Figure 2a).

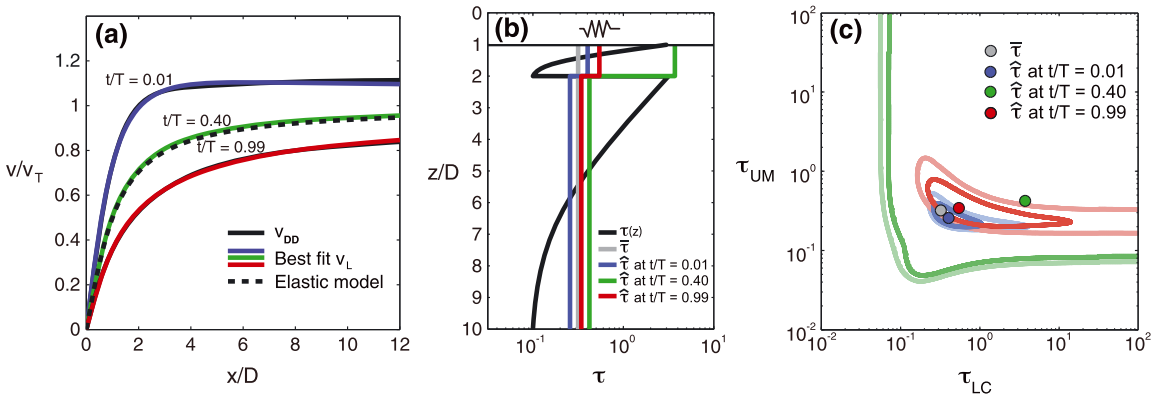

Figure 2. (a) Velocities for a depth-dependent model, v_{DD} (black solid lines) and the best fitting velocities predicted by a layered model, v_L (colored solid lines). Black dashed line is the velocities predicted by an elastic earthquake model with the same D and v_T. (b) τ profiles corresponding to v_{DD} and $\hat{\tau}_j$ associated with the best fitting v_L in Figure 2a. (c) $\bar{\tau}_j$ for the τ profile with $\hat{\tau}_j$ for each of the cases in Figure 2b. Solid lines indicate misfit contours in the grid-search estimation of v_L in Figure 2a; contours shown are RMSE = 0.02 (dark lines) and 0.04 (faded lines), and color indicates the time.

Because all models simultaneously predict surface interseismic velocities similar to the elastic model, $\hat{\tau}_j$ cannot be definitively resolved for a period during the middle of the earthquake cycle (Figure 3c). The exact time within the earthquake cycle in which the elastic model describes v_{DD} as well as a layered model depends on the specific τ profiles, but it is during the time period about $0.4T$–$0.5T$ for most of the models.

[9] In general, the misfit between v_{DD} and v_L is largest early in the earthquake cycle for models with low $\bar{\tau}_{LC}$ and/or $\bar{\tau}_{UM}$ (Figure S2). The heightened misfit reflects the fact that there is more postseismic creep in the midcrust and/or beneath the Moho in the layered models, resulting in differences in the wavelength of surface deformation compared to the depth-dependent models in which τ is larger in the midcrust and/or beneath the Moho. Misfit decreases to a minimum halfway into the earthquake cycle when deformation appears elastic. The misfit increases again late in the earthquake cycle, although v_L is a significantly better match to v_{DD} compared to immediately after the earthquake.

[10] We illustrate the determination of $\hat{\tau}_j$ using a model with a depth-dependent τ profile such that $\bar{\tau}_{LC} = \bar{\tau}_{UM} = 10^{-0.5}$, $\tau_{LC}^{\max} = \tau_{UM}^{\max} = 10^{0.5}$, and $\tau_{LC}^{\min} = \tau_{UM}^{\min} = 10^{-1}$ (Figure 2). For this particular case, the misfit surfaces in the grid search shows clear minima and $\hat{\tau}_j$ is a fair approximation for $\bar{\tau}_j$ early and late in the interseismic period, although the lower crust relaxation time is slightly overestimated (Figure 2c). About halfway into the cycle, the layered model that best fits v_{DD} dramatically overestimates the lower crust relaxation time (Figure 2b); however, there is a large range of $\hat{\tau}_j$ that would sufficiently match v_{DD} (Figure 2c), since during this period, the surface velocities for all models are very close to the velocities for the elastic model with identical fault slip rate and locking depth (Figure 2a). In this particular depth-dependent model, the velocities throughout the interseismic period are quite similar to those from elastic models, albeit with different slip rates and locking depths.

4. Biases in Apparent Strength

[11] One might assume that the apparent τ estimated using a simple layered model, $\hat{\tau}_j$, reflects the geometric mean τ in those layers, $\bar{\tau}_j$. In general, $\hat{\tau}_j$ estimated from v_{DD} at any time in one of the depth-dependent models may be significantly different than $\bar{\tau}_j$. We consider the difference between the two values to be an error in the estimation of $\bar{\tau}_j$ and approximate the bias in the estimation throughout the interseismic period as

$$\text{Bias}(\hat{\tau}_j; \bar{\tau}_j) = E[\hat{\tau}_j] - \bar{\tau}_j, \tag{2}$$

where $E[\hat{\tau}_j]$ is the geometric mean of $\hat{\tau}_j$ estimated from the collection of the depth-dependent models that all have the same $\bar{\tau}_j$.

[12] $\text{Bias}(\hat{\tau}_j; \bar{\tau}_j)$ represents the bias in the estimated relaxation times for the lower crust and uppermost mantle with respect to the geometric mean relaxation time of the two layers. In the wide range of models we considered, the bias depends on the contrast between the geometric mean relaxation times in the lower crust and upper mantle, $\bar{\tau}_{LC}/\bar{\tau}_{UM}$. Early and late in the earthquake cycle there is a distinct bias toward an apparently weak upper mantle when $\bar{\tau}_{LC}/\bar{\tau}_{UM} < 1$ and a bias exaggerating the strength of the lower crust by up to a few orders of magnitude when $\bar{\tau}_{LC}/\bar{\tau}_{UM} > 1$ (Figures 3a and 3c). About halfway through the interseismic period, the biases we calculate are not well constrained, but are generally toward a stronger lower crust and uppermost mantle (Figure 3b). These biases hold when we only consider τ profiles in which τ decays with depth faster than log linearly (Figure S4), which indicates the biases are not sensitive to the specific decay of viscosity with depth provided that there is still some depth dependence within both layers.

[13] When we consider models in which the lower crust is homogeneous and include a depth-dependent τ only in the uppermost mantle, there is no clear bias when $\bar{\tau}_{LC}/\bar{\tau}_{UM} < 1$. However, when $\bar{\tau}_{LC}/\bar{\tau}_{UM} > 1$, there is a bias to a stronger lower crust and only a slight bias in the upper mantle strength (Figures 3a and 3c). Conversely, when the uppermost mantle has a uniform relaxation time and τ is depth dependent only in the lower crust, there is no bias when $\bar{\tau}_{LC}/\bar{\tau}_{UM} > 1$, but when $\bar{\tau}_{LC}/\bar{\tau}_{UM} < 1$, there is a bias toward a weaker upper mantle, while the lower crust relaxation time is accurately represented (Figures S3d and S3f). This may be counterintuitive, as one might think that if the lower crust or mantle was truly homogenous with respect to its

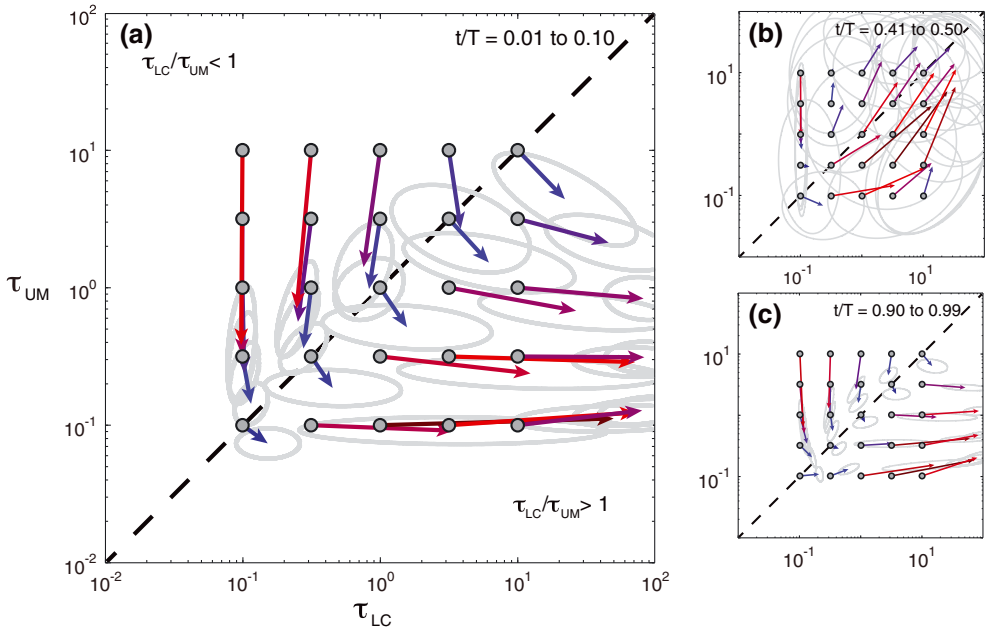

Figure 3. $\bar{\tau}_j$ for all depth-dependent τ models considered (gray dots), along with the estimation Bias($\hat{\tau}_j$; $\bar{\tau}_j$) (vectors) (a) early, (b) midway, and (c) late in the interseismic period. Each vector points to the mean $\hat{\tau}_j$ estimated from depth-dependent models with the same $\bar{\tau}_j$, and the gray ovals indicate one standard deviation of $\hat{\tau}_j$. The vector colors reflect the magnitude of the bias and help to distinguish overlapping vectors.

relaxation time, then a simplified layered model should accurately capture that uniform relaxation time. In the case of both the lower crust and uppermost mantle being homogeneous, this would be true. However, if only one layer has a homogeneous relaxation time which is longer than the mean relaxation time in the depth-dependent layer, then strength estimates for that layer are biased. This leads us to conclude that the biases are created by the depth dependence of τ in the weaker of the two ductile lithospheric layers.

5. Lower Crustal Shear Zones

[14] It is likely that highly sheared rocks directly beneath a fault are considerably weaker than the surrounding lower crust [e.g., *Montési and Hirth*, 2003] and lower crustal shear zones are well documented [e.g., *Vauchez and Tommasi*, 2003]. In all of the models that we present above, the largest τ in the lower crust is immediately beneath the fault. These long relaxation times may suppress the relaxation of coseismic stresses in the lowermost crust, where the relaxation times are shorter, and thus may significantly influence our above conclusion that estimates of lower crustal strength are biased to stronger values than its geometric mean strength. To investigate the potential effect of a lower crustal shear zone on the biases in $\hat{\tau}_j$, we include a D wide vertical shear zone extending through the lower crust beneath the fault. We assume that the shear zone is Maxwell viscoelastic with a constant relaxation time of $\tau_{SZ} = 10^{-2}$, which is at least an order of magnitude faster than the surrounding lower crust.

[15] With a weak shear zone, immediately following an earthquake, the velocities are quite large, and as a result, both the lower crust and uppermost mantle appear uniformly weaker than their geometric mean strength, with $\hat{\tau}_{LC}$ close to τ_{SZ} (Figure 4). These heightened postseismic velocities decay rapidly, although how $\hat{\tau}_{LC}$ or $\hat{\tau}_{UM}$ increases over time depends on $\bar{\tau}_{LC}/\bar{\tau}_{UM}$. If $\bar{\tau}_{LC}/\bar{\tau}_{UM} > 1$, then $\hat{\tau}_{LC}$ increases by orders of magnitude, exceeding $\bar{\tau}_{LC}$ (Figure 4b). Otherwise, $\hat{\tau}_{UM}$ rapidly increases early in the cycle. For all models, $\hat{\tau}_j$ evolves toward a more reasonable approximation of $\bar{\tau}_j$ late in the cycle (Figure 4b). Additionally, the velocities are relatively steady throughout the later interseismic period compared to a model without a shear zone but with similar heightened postseismic velocities (Figure 4a).

6. Discussion

[16] In the wide range of cases we consider, the biases in $\hat{\tau}_j$ inferred throughout the interseismic period almost always are such that $\hat{\tau}_{LC}/\hat{\tau}_{UM}$ is larger than $\bar{\tau}_{LC}/\bar{\tau}_{UM}$, except for midway through the interseismic period when all velocities are close to the elastic limit (Figure 3b). Additionally, $\hat{\tau}_{LC}$ is often larger than $\tau_{LC}^{\max}$ and $\hat{\tau}_{UM}$ is often lower that $\tau_{UM}^{\min}$. In models where $\bar{\tau}_{LC} \neq \bar{\tau}_{UM}$, inferences of $\hat{\tau}_{LC}/\hat{\tau}_{UM} > 1$ (< 1) correspond to models in which $\bar{\tau}_{LC}/\bar{\tau}_{UM} > 1$ (< 1). In other words, a lower crust that appears stronger than the mantle when approximated by uniform strength layers corresponds to models in which the geometric mean strength of the lower crust is also stronger than that in the mantle, and *vice versa*. We note that several of the τ profiles with $\bar{\tau}_{LC} > \bar{\tau}_{UM}$ are characterized by significant portions of the lowermost crust having much lower viscosities than the uppermost mantle.

[17] The biases we present in this paper can be viewed as relating $\hat{\tau}_j$ to $\bar{\tau}_j$. However, the specific relationship between $\hat{\tau}_j$ and $\bar{\tau}_j$ depends not only on the details of how τ varies in the ductile lithosphere but also on the time in the interseismic period. In the latter regard, it is also important to note that we have assumed periodic offsets on an infinite length fault, whereas real earthquakes are nonperiodic and finite. It is also important to note that we grouped all τ profiles according to the $\bar{\tau}_j$ in each layer irrespective of

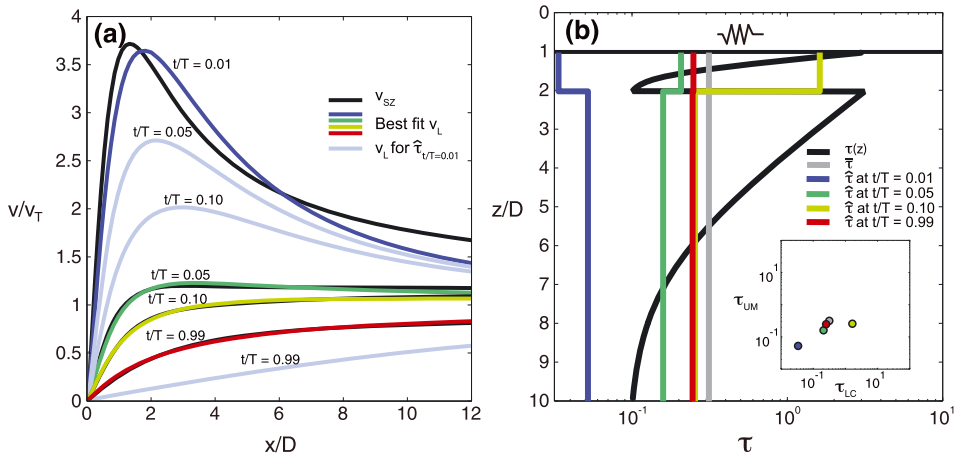

Figure 4. (a) Interseismic velocities, v_{SZ}, in a model with both a lower crustal shear zone and depth-dependent τ in the surrounding lithosphere (black lines) along with the best fit v_L (colored lines). Shown as light blue lines are the velocities in a layered model with the dark blue viscosity profile shown in Figure 4b, which are the apparent viscosities estimated from v_{SZ} at $t/T = 0.01$. (b) τ profile outside of the shear zone corresponding to v_{SZ} (black line; $\tau = 10^{-2}$ within the shear zone), $\bar{\tau}$ outside the shear zone, and $\hat{\tau}_j$ associated with the best fitting v_L in Figure 4a (colored lines, color corresponds to time in cycle). Inset in Figure 4b shows $\bar{\tau}_j$ and $\hat{\tau}_j$ (dot color corresponds to line colors in Figures 4a and 4b).

$\tau_j^{\max}$ and $\tau_j^{\min}$, and only considered how profiles with the same $\bar{\tau}_j$ relate to $\hat{\tau}_j$. For these reasons, these biases cannot be used to back out specific depth-dependent τ profiles, or even unique $\bar{\tau}_j$, consistent with $\hat{\tau}_j$ estimated from geodetic data using a simplified model of the lithosphere. The coherency of the bias estimates suggest that it may be possible to develop probabilistic relationships between $\hat{\tau}_j$ and $\bar{\tau}_j$, assuming that the general time within the earthquake cycle the geodetic data are sampling is known. For example, if $\hat{\tau}_{LC} \approx 10^{1}$ and $\hat{\tau}_{UM} \approx 10^{-1}$ were inferred from geodetic data late in a seismic cycle, then those estimates would be equivalent to depth-dependent τ profiles with $\bar{\tau}_{LC}$ around $10^{-0.5}$ to 10^{1} and $\bar{\tau}_{UM}$ on the order of 10^{-1} (Figure 3c). Further exploration of the relationships between specific τ profiles and $\hat{\tau}_j$ would be required in order to establish whether inferences of apparent strength could be used to constrain the range of permissible τ profiles that are consistent with surface deformation at any one time. It may also be possible to constrain depth-dependent τ profiles by considering how inferred viscosities vary as a function of distance from the fault [*Yamasaki and Houseman*, 2012a].

[18] In the depth-dependent τ models we consider, the postseismic velocities are either only slightly above the elastic velocities or are large but decay over a relatively long portion of the interseismic period. Both of these cases are in contrast with many observations of heightened postseismic velocities decaying over on order of a decade following earthquakes [e.g., *Ergintav et al.*, 2009]. Models including transient rheologies or power law creep have been proposed to explain transient postseismic velocities [e.g., *Pollitz*, 2003; *Freed et al.*, 2006; *Ryder et al.*, 2007]. Adding a weak shear zone to a model with depth-dependent τ and only Maxwell viscoelasticity can also result in heightened postseismic velocities that rapidly decay over the postseismic period, while the surface velocities throughout the majority of the latter interseismic period are only slightly depressed compared to those in an elastic model with identical slip rate and locking depth (Figure 4a).

7. Conclusions

[19] Assuming a uniform viscosity for the lower crust and uppermost mantle results in biased estimates of viscosity for those two layers if the viscosity is highly depth-dependent. Estimates of viscosity tend to be biased either toward a weaker upper mantle or a stronger lower crust, depending on the relative viscosity of the two layers. When there is a low viscosity lower crustal shear zone present, immediately after the earthquake the lower crust and uppermost mantle both appear weak, with apparent viscosities close to that of the shear zone, and then the apparent strength of the lower crust or upper mantle increases dramatically over the early interseismic period. Using simplified models, inferences made from interseismic deformation that the lower crust is orders of magnitude more viscous than the upper mantle may be entirely consistent with depth-dependent viscosity profiles that have smaller contrasts between the geometric mean viscosities of the lower crust and upper mantle and may be associated with a significant increase in viscosity across the Moho.

[20] **Acknowledgments.** This research was funded by NSF grant EAR 1045372. We thank editor E. Calais, G. Houseman, and an anonymous reviewer.

[21] The Editor thanks two anonymous reviewers for their assistance in evaluating this paper.

References

Bürgmann, R., and G. Dresen (2008), Rheology of the lower crust and upper mantle: Evidence from rock mechanics, geodesy, and field observations, *Annu. Rev. Earth Planet. Sci.*, *36*, 531–567.

Ergintav, S., S. McClusky, E. Hearn, R. Reilinger, R. Cakmak, T. Herring, H. Ozener, O. Lenk, and E. Tari (2009), Seven years of postseismic deformation following the 1999 M = 7.4 and M = 7.2 İzmit-Düzce, Turkey earthquake sequence, *J. Geophys. Res.*, *114*, B07403, doi:10.1029/2008JB006021.

Freed, A. M., R. Bürgmann, E. Calais, and J. Freymeuller (2006), Stress-dependent power-law flow in the upper mantle following the 2002 Denali, Alaska, earthquake, *Earth Planet. Sci. Lett.*, *252*, 481–489.

Hearn, E., S. Ergintav, McClusky S., and R. Reilinger (2009), İzmit earthquake postseismic deformation and dynamics of the North Anatolian Fault Zone, *J. Geophys. Res.*, *114*, B08405, doi:10.1029/2008JB006026.

Hetland, E. A., and B. H. Hager (2003), Postseismic relaxation across the Central Nevada Seismic Belt, *J. Geophys. Res.*, *108* (B8), 2394, doi:10.1029/2002JB002257.

Johnson, K. M., G. E. Hilley, and R. Bürgmann (2007), Influence of lithosphere viscosity structure on estimates of fault slip rate in the Mojave region of San Andreas fault system, *J. Geophys. Res.*, *112*, B07408, doi:10.1029/2006JB004842.

Kohlstedt, D. L., B. Evans, and S. J. Mackwell (1995), Strength of the lithosphere: Constraints imposed by laboratory experiments, *J. Geophys. Res.*, *100*, 17587–17602.

Lyzenga, G. A., W. R. Panero, and A. Donnellan (2000), Influence of anelastic surface layers on postseismic thrust fault deformation, *J. Geophys. Res.*, *105*, 3151–3157.

Meade, B. J., Y. Klinger, and E. A. Hetland (2013), Inference of multiple earthquake cycle relaxation time scales of interseismic deformation, *Bull. Seismol. Soc. Am.*, in press.

Montési, L., and G. Hirth (2003), Grain size evolution and the rheology of ductile shear zones: From laboratory experiments to postseismic creep, *Earth Planet. Sci. Lett.*, *211*, 97–110.

Pollitz, F. F., and W. Thatcher (2010), On the resolution of shallow mantle viscosity structure using postearthquake relaxation data: Application to the 1999 Hector Mine, California, earthquake, *J. Geophys. Res.*, *115*, B10412, doi:10.1029/2010JB007405.

Pollitz, F. F. (2003), Transient rheology of the uppermost mantle beneath the Mojave Desert, California, *Earth Planet. Sci. Lett.*, *215*, 89–104.

Pollitz, F. F. (2005), Transient rheology of the upper mantle beneath central Alaska inferred from the crustal velocity field following the 2002 Denali earthquake, *J. Geophys. Res.*, *110*, B08407, doi:10.1029/2005JB003672.

Riva, R. E. M., and R. Govers (2009), Relating viscosities from postseismic relaxation to a realistic viscosity structure for the lithosphere, *Geophys. J. Int.*, *176*, 614–624.

Ryder, I., B. Parsons, T. J. Wright, and G. J. Funning (2007), Post-seismic motion following the 1997 Manyi (Tibet) earthquake: InSAR observations and modelling, *Geophys. J. Int.*, *169*, 1009–1027.

Savage, J. C., and R. O. Burford (1973), Geodetic determination of relative plate motion in central California, *J. Geophys. Res.*, *78*, 832–845.

Savage, J., and W. Prescott (1978), Asthenosphere readjustment and the earthquake cycle, *J. Geophys. Res.*, *83*, 3369–3376.

Thatcher, W., and F. F. Pollitz (2008), Temporal evolution of continental lithospheric strength in actively deforming regions, *GSA Today*, *18*, 4–11, doi:10.1130/GSAT01804-5A.1.

Vauchez, A., and A. Tommasi (2003), Wrench faults down to the asthenosphere: geological and geophysical evidence and thermomechanical effects, *Geol. Soc. Spec. Publ.*, *210*, 15–34.

Yamasaki, T., and G. Houseman (2012a), The signature of depth-dependent viscosity structure in post-seismic deformation, *Geophys. J. Int.*, *190*, 769–784, doi:10.1111/j.1365-246X.2012.05534.x.

Yamasaki, T., and G. Houseman (2012b), The crustal viscosity gradient measured from post-seismic deformation: A case study of the 1997 Manyi (Tibet) earthquake, *Earth Planet. Sci. Lett.*, *14*, 351–352.